教育部公費留學生博士後及短期研究人員成果報告書

省力最佳化輪椅研究

公費生姓名：郭藍遠

出國地點：美國 Mayo Clinic,
Orthopaedic Biomechanics Lab

出國期間：06/02/01~03/22/02

報告日期：03/29/02

編　　號　　欄

出國人員

郭藍遠

國立成功大學 醫學工程研究所

摘要

在台灣，工業局統計報告我國醫療器材1997年出口總額為2億4600多萬美元。出口項目佔第一位為輪椅及其零件，金額7000多萬美元，其中手動輪椅佔約70%。腕關節、肩關節及其他上肢部位受傷是手動輪椅使用者最常見的問題，但很少文獻探討有關手推輪椅的生物力學。特別是探討其中上肢的受力與骨骼肌肉問題之間關係的研究，更是罕見。

從過去一系列的研究中顯示腕關節症候群及肩關節疼痛的主要是在驅動輪椅時上肢關節承受了高的負荷。然而，輪椅驅動時，低機械效率(大約10%)的原因仍未知。對機械能量問題深入分析探討，對能量如何轉換產生肢體活動進一步了解，將可幫助預測如何產生最大機械效能。因此，本研究計劃重點項目為發展更進一層的能量模型來評估軀幹或上肢的機械能和功率；探討上肢各肢段的功率流動與機械功率。另外，因為輪椅推動之變異性很大，如受測者的技巧等等；常使得輪椅結構的細微改變，無法用客觀的實驗來印證。因此我們發展了一套數學最佳化分析方法，以上肢各肢體長度為已知，利用四連桿(four bar linkage)原理來估計上之各關節再輪椅推動時的位置和角度；並利用輪椅推動力量之向量為未知；並配合上肢各關節的肌肉之最大力量為限制，來決定出達到最大輪椅前進力矩的最佳輪椅推動力量之向量。利用最佳化分析來預測，在上肢關節計測資料與肌力限制下，如何產生相對於輪軸之最大前進力矩和最大機械效能，該研究成果印證與實驗表現結果相仿。

經由此研究，由分析驅動技巧之結果，將可作為加強傷害防護、輪椅設計及肌肉骨骼傷害之復健治療等的參考。同時，藉由驅動效率的改進，將有助於降低輪椅長期使用者受傷的機率，以增加輪椅使用者的獨立性，使其方便於參加社會上的各種團體活動。此外，本研究的方法及技術將引進國內並轉移至台灣的輪椅製造商，以助於國產醫療產品之國際化。

目次

目的

手/腕關節問題，肩關節疼痛和其他的上肢受傷都是手推輪椅常見的健康問題； 主訴為腕隧道症候群和肩關節疼痛。儘管使用輪椅者好發上肢肌肉與骨骼的問題有的比例非常高，但卻很少關於輪椅驅動的生物力學研究資料存在；特別是針對上肢負荷和肌肉與骨骼問題間的關係更是少見探討。此外，為什麼輪椅驅動的機械效率低於10%的原因，仍然不清楚。相較之下，手搖輪椅機械效率為大約 15%，腳踏車約為20%，單獨肌肉收縮約為30%，都較手推輪椅來得高。過去機械能量和功率流的分析在步態分析有極好研究，但據我們所知機械能量和功率流的分析在輪椅驅動方面的探討，並未有任何相關研究報告提出。如果沒有動力學方面的知識，我們就不知道我們觀察的動作是如何產生的。而正確機械功的計算，對我們評估輪椅驅動時的機械效率是非常重要的。

本篇研究計劃之主要目標為基於人體測量學、經驗和輪椅使用者的身體損害來建立架構手推輪椅的個別化方針，這些個別化方針將改善手推輪椅驅動效率和減少上肢受傷的機會。為了達到此目的，輪椅驅動的研究不僅需評估上肢的負荷力，同時評估輪椅驅動時上肢的機械能和功率流，也是相同重要。上肢骨骼肌肉系統提供的功率若與觀察到的動作所需要的功率之間差異越小，輪椅驅動的機械效率就會越高。

輪椅推動之變異性很大，如受測者的技巧等等；常使得輪椅結構的細微改變，無法用客觀的實驗來印證。因此我們發展了一套數學最佳化分析方法，以上肢各肢體長度為已知，利用四連桿(four bar linkage)原理來估計上之各關節再輪椅推動時的位置和角度；並利用輪椅推動力量之向量為未知；並配合上肢各關節的肌肉之最大力量為限制，來決定出達到最大輪椅前進力矩的最佳輪椅推動力量之向量。利用最佳化分析來預測，在上肢關節計測資料與肌力限制下，如何產生相對於輪軸之最大前進力矩和最大機械效能。

經由此研究，由分析驅動技巧之結果，將可作為加強傷害防護、輪椅設計及肌肉骨骼傷害之復健治療等的參考。同時，藉由驅動效率的改進，將有助於降低輪椅長期使用者受傷的機率，以增加輪椅使用者的獨立性。

Mayo Clinic, MN, USA 是美國首屈一指的醫學中心，它的 Orthopaedic Biomechanics Laboratory 為世界上最出名的的生物力學實驗室，尤其在動態分析方面相關之研究更是著名。該實驗室在輪椅推動生物力學上的研究是非常傑出與精進，已發表數篇論文在非常著名的工程和臨床醫學期刊上，為此相關研究的重要研究機構。Dr. An 是世界知名的生物力學學者，已發表超過四百篇論文於知名的 SCI 期刊，同時也是許多知名期刊的編輯。Dr. An 在與輪椅推動息息相關的上肢生物力學研究更是專門，是該領域的國際級大師；已發表數篇論文在非常著名的工程和臨床醫學期刊上，僅列出其中幾篇。其與申請者之指導教授 蘇芳慶教授正進行國家衛生研究院有關輪椅生物力學分析之計劃合作，

關係非常密切。希望將此相關的理論與技術應用在輪椅推動分析上；並且帶回國內，提昇此方面研究的水平。

過程

筆者赴美後立刻至申請之實驗室報到，並進行相關研究工作。由於指導教授 Dr. An **手邊正執行一個美國國家研究院**(NIH)**關於輪椅推動生物力學方面的研究計劃，因此筆者可以在模型建立與實驗等工作都能很順利的進行。**

筆者首先是延續在成大之主題，將輪椅能量模型建立，並完成論文書寫，且投稿至 Clinical Biomechanics.(SCI **期刊，附件一)；已被列為可接受，正在修改中。**Dr. An **給我的主要任務是以發展輪椅驅動模式，並加以相關實驗來印證此模式的正確性。而實驗部分，由於實驗工作已有該實驗室的正式員工執行，因此筆者之工作以分析資料為主。至今，輪椅驅動模式部份已投稿一篇至** Disability and Rehabilitation(SCI **期刊**);**另外也完成一篇論文繕寫(附件二)，在所有作者都看過後，將立刻投稿至國際知名期刊。**

能量模型

機械能

動能：**對一個物體作功的效果是增加其能量，能量變化的數量是與在物體上所作的功相同，並以相同的單位表示。物體運動產生的能量稱之為動能**

由公式計算

$E_k = 1/2\ mv^2 + 1/2\ (I_{x'}\ w_{x'}^2 + \quad I_{y'}\ w_{y'}^2 + \quad I_{y'}\ w_{y'}^2)$

其中 $v = \sqrt{v_x^2 + v_y^2 + v_z^2}$

這裡， Ek **表示動能，**m**是質量，**v**是物體的速度，**I**是物體沿主要慣性軸** (x' **、** y'**、** z') **相應的慣性質量，**w **是物體的角速度。這樣，所有的速度皆與動能相關，一個物體的總和動能將包括平移和旋轉兩部分。**

平移和旋轉運動一個物體，所作的功為

$W = \mathbf{F} \cdot \mathbf{s} + \boldsymbol{M} \cdot \boldsymbol{q}$

功率為

$P = \mathbf{F} \cdot \mathbf{v} + \boldsymbol{M} \cdot \boldsymbol{w}$

位能： **由重力產生主要的位能。可以想像它的影響就像一個隱形彈簧，存在於物體中心和地球中心，並總是向下拉。所以要向上使這個物體移動，就需做功，並貯存在伸開的彈簧中。同樣地，當減少物體高度時，能夠使存儲的潛在能量轉變成動能。累積的位能變化等於升高距離**×**重力：**

$\Delta E_p = s\ g$

一個物體的總機械能是它的位能和動能的總和。

驅動輪椅時，身體的總機械能量並未守恆。驅動輪椅所需的能量和不同類型能量間的折中是本篇研究的目的。 經由總和軀幹與兩上臂的能量，忽略骨盆和兩下肢，機械能量將可被計算和分析。
能量的變化率將被計算出，來代表輪椅驅動時的功率需求。

上肢的功率平衡
在上面討論的肢段的功率需求是從機械能量變化率計算得到；可以與由關節合力和肢段速度計算求得的流進和流出功率的不同方法來作比較。

想像肢段是一個獨立自由地運動物體。有力和力矩施在任一個末端。這末端相對某一外界參考座標將產生平移速度，並且可能也有旋轉速度。此外，肢段質量中心有相同其重量的力，如果物體有轉動，質量中心的平移速度將不同於肢段末端。從物體某一個末端的得到或失去的功率等於關節淨合力與關節平移速度的內積加上關節淨合力矩與物體旋轉速度(不是關節旋轉速度)的內積。特別注意力與力矩必須與肢段速度表示在同一座標系統。所有關節的功率流與重力所產生的功率的總和代表此肢段的總功率。

$$P_f = \mathbf{F_d} \cdot \mathbf{v_d} + \boldsymbol{M_d} \cdot \boldsymbol{w_d} + \mathbf{F_p} \cdot \mathbf{v_p} + \boldsymbol{M_p} \cdot \boldsymbol{w_p} + \mathrm{mg}v_y$$

肢段的總功率的積分可用來估計此肢段的能量。

上肢的總功率流(TPF)為

$$TPF = P_{f\text{-}upper} + P_{f\text{-}foream} + P_{f\text{-}hand}$$

這兩個功率估計之間的差異，在輪椅驅動時是能量消耗的重要指標。最理想驅動技術和輪椅的設計，是試圖使能量消耗減到最低。

驅動機械效能的分析模式

受測者輪椅驅動表現變異性很大，使得輪椅結構細微的改變，無法用客觀的實驗來印證。因此我們發展了一套數學最佳化分析方法，提供一個更深度了解輪椅設計以及更系統的，參數方式地探討輪椅設計對輪椅驅動機械效能的影響的；並且是一個探討輪椅驅動時，上肢與軀幹的分析模型(圖一)。這個模型將逐步被發展，最後幾近於理想。應用於此模型的初始假設將逐步放鬆或者修改使得與實驗測量分析結果的比較接近。

輪椅驅動包含完整的上肢與軀幹的三度空間運動。 然而，在初始模型發展方面， 我們感覺到集中於探討最主要的運動平面-矢狀面，就已經足夠。初始模型發展 將考慮肩關節彎曲/伸直，肘關節彎曲和伸直和腕關節的橈側和尺側彎曲。此模型是以上肢各關節

的運動位置為已知，輪椅驅動力量之向量為未知；並配合上肢各關節的肌肉之最大力量為限制，來決定出整個驅動週期中，達到最大輪椅前進力矩的最佳輪椅驅動力量之向量。

Maximize M_r

Subject to：

$M_s = \mathbf{P}_s \times \mathbf{F}_h$

$M_e = \mathbf{P}_e \times \mathbf{F}_h$

$M_w = \mathbf{P}_w \times \mathbf{F}_h$

$M_r = \mathbf{P}_r \times \mathbf{F}_h$

$-M_{se} \le M_s \le M_{sf}$

$-M_{ee} \le M_e \le M_{ef}$

$-M_{wu} \le M_w \le M_{wr}$

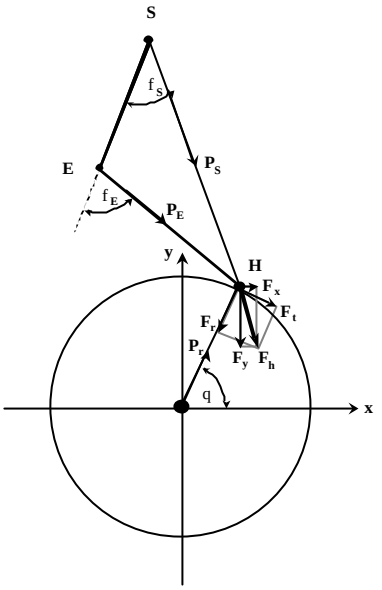

圖一、輪椅驅動的分析模型。

其中未知的變數Fh**為輪椅驅動力量的向量，包含**Ft**和**Fr**兩部分。**Ft **是施於輪圈力量的切線力量部分，**Fr**是施於輪圈力量的向軸心力量部分。**Ms**和**Me**是由**Fh**施於輪圈所產生於肩關節和肘關節的彎曲/伸展力矩。**Mw**是由**Fh**施於輪圈所產生於腕關節的橈側/尺側彎曲力矩。**Mr**是由**Fh**施於輪圈所產生的輪椅前進力矩。**

Mss**和**Msf**是肩關節在伸展和彎曲方向最大肌力值；**Mee**和**Mef**是肘關節在伸展和彎曲方向最大肌力值；**Mwu **和**Mwr**是腕關節的橈側和尺側彎曲方向最大肌力值。**Ps、Pe、Pw、Pr**是肩關節、肘關節、腕關節、輪軸相對於力在輪圈的接觸點的位置向量。**

心得

赴美學習前雖已深信此行將收獲良多，現在回想過真如此；但當時心中難免有諸多忐忑不安，部分是來自於將面對陌生環境、語言與人種的不確定感。非常幸運地，一到 Mayo 骨科生物力學實驗室後，即受到指導教授 Dr. An 的親切照顧。他真是一位非常和藹的長者；他不斷關心我的研究工作進行，對於同行的家人小孩，也熱切關懷，令筆者感受深刻。Dr. An 雖然已經在國際生物力學界為大師級人物，但卻一點架子也沒有，是我一生中碰到過最好的人之一了。每星期我都有機會和忙碌異常的 Dr. An 開會一次，討論上週完成的工作與未來的一週工作事項；這些都是使我能順利完成工作，並有豐碩成果的最大原因。事實上整個研究工作並不是一帆風順，其中我們也遭遇到模式結果無法與文獻配合的窘境，而困住一段時間，但 Dr. An 務實地要求我從最基礎的實驗中一步步印證，最後都能將模式結果，在實驗中得到印證，算是此方面研究的重大突破。也因為此過程，讓我有機會親身體會大師級人物在面對難題時分析問題的邏輯與態度，真是非常可貴的經驗。

在美國一年，親身體驗其實驗室的運作，印象最深刻是其專業分工與管理制度。在該實驗室中實驗資料抓取有專門的物理治療師(physical therapy)或肌動學專家(kinesiologist)負責，程式有特別的程式師(programmer)編寫，而實驗設備修改與製造有專門之工程師(engineer)負責，行政工作有數個秘書(sectary)負責，整個實驗室管理也有一位監督(supervisor)負責。實驗室主任(director)，相關醫師(medical doctor) 和博士後研究員(post doctoral research fellow) 負責提出研究計劃申請經費、分析資料、並撰寫論文發表等工作。大家有各自工作，沒有一個人能獨當一面完成所有任務；因此他們也非常強調團隊合作的重要性。反觀，在台灣的研究生都必須獨立完成整個研究計劃中之大部分任務，雖可有較多之訓練，但在重要之研究之突破與創新，常因為力不從心而有缺憾之現象。而其管理制度之綿密與完整也是我不得佩服之處，舉凡文具申請，空間擺置與清潔，設備之維護等等都可看出其制度建立之完善。

在美國期間，不幸地遇上恐怖份子攻擊世貿大樓的 911 事件，讓家人非常擔心；雖然所居住的地區，非常安全，但後繼的 anthrax 郵包白色粉末事件，及美國國安全局一連串的恐怖攻擊預警還是讓人提心吊膽。所幸教育部國際文教處立即發表相關注意事項，給在外的留學生參考，讓我們有所準則加以因應，安心不少。

最後，筆者願意對跟隨近六年的指導教授蘇芳慶教授，表達最深的謝意。他對筆者此次申請出國進修，一直表達積極支持之意，這是我能成行之最大根本原因。

建議

教育部應多增加名額提供國內博士班學生出國進修

國內博士班研究所已越來越多，而其課程也越來越完善，甚至可以比美許多先進國家的博士班課程；因此許多優秀的青年學子在經濟考量下，願意選擇留在國內修博士班。但畢竟許多大師級人物都是待在國外的大學或實驗室中，如果能有機會親臨學習，將是非常寶貴的經驗；而且在國外環境中可以讓你擴展視野、學習語言、了解不同國家和不同實驗室的運作模式，這些都是非常重要的經驗。

延長研究年限至兩年

現行規定一年期間稍嫌太短，因為初到一個陌生實驗室，從摸索到真正能開始進行研究，需要為期一段時間；而等全部都上軌道，通常已距返國時日非常近了。在國外實驗室中發現日本來研究人員都是以停留兩年為計劃，因為他們普遍都有此觀念，假設一年可產一篇論文，那兩年至少可產三篇以上論文，道理同上所述。

指導教授之心態

筆者此次能順利成行，最大根本原因是有指導教授的支持。若眾多博士班學生的指導教授們皆有此開放心態，相信對國際學術交流與合作將會有諸多幫助。

附件

Mechanical Energy and Power Flow of the Upper Extremity in Manual Wheelchair Propulsion

Lan-Yuen Guo*†, M.S., PT, Fong-Chin Su*, Ph.D., Hong-Wen Wu**, Ph.D., Kai-Nan An‡, Ph.D.

**Institute of Biomedical Engineering, National Cheng Kung University, Tainan, Taiwan*
†Department of Physical Therapy, Tzu Chi College of Technology, Hualian, Taiwan
***Department of Physical Therapy, China College of Medicine, Taichung, Taiwan*
‡Orthopaedic Biomechanics Laboratory, Mayo Clinic/May Foundation, Rochester, MN, USA

Nov 2001

ADDRESS CORRESPONDENCE AND REPRINT REQUESTED TO

Fong-Chin Su, Ph.D.
Institute of Biomedical Engineering
National Cheng Kung University
Tainan, 701
TAIWAN
Tel: 888-6-2760665
Fax: 886-6-2343270
Email: fcsu@mail.ncku.edu.tw

Running head: Energy and Power in Manual Wheelchair

Abstract

Objective. To investigate the characteristics of mechanical energy and power flow of the upper limb during wheelchair propulsion.

Design. Mechanical energy and power flow of segments were calculated

Background. No studies have taken into account the mechanical energy and power flow of the musculoskeletal system for wheelchair propulsion. These mechanical energy and power flow study was proved to be a useful tool for investigating the locomotion disorder during human walking.

Methods. Twelve young normal male adults (mean age 23.5 years old) were recruited for this study. Both 3-D kinematic and kinetic data of upper extremity in wheelchair propulsion were collected by the Hi-Res Expert Vision system and by an instrumented wheel, respectively.

Results. During initial propulsion phase, the joint power flow is generated in the upper arm or is transferred from the trunk downward to forearm/hand to propel the wheel forward. During the terminal propulsion, the joint power flow is transferred upward to the trunk from the forearm and upper arm. The rate of change of mechanical energy and power flow show a similar pattern for the forearm and hand, but there is larger discrepancy for the upper arm.

Conclusions. The joint power play an important role for energy transfer as well as the muscle generate and absorbing energy between segments during wheelchair propulsion.

Relevance

The energetic information allows us to gain a better understanding of the role of musculoskeletal system act during wheelchair propulsion

Key Words: Wheelchair; Biomechanics; Movement; Kinetics

Introduction

That handrim wheelchair propulsion is indeed strenuous which is inferred from its low mechanical efficiency. The gross mechanical efficiency in wheelchair propulsion rarely rises above 10% [1]. Hand/wrist problem, shoulder pain and other upper extremity injuries are well-known health problems in relation to manual wheelchair propulsion. Despite the high incidence of upper extremity musculoskeletal problems among individuals relying on wheelchairs, few published data exists regarding the biomechanics of wheelchair propulsion. In addition, the reason of low mechanical efficiency associated with wheelchair propulsion is still not clear. In past, the energy cost during wheelchair propulsion was measured by physiological technique i.e. collecting the amount of oxygen consumption during activity [1-4]. While the results of these studies have proven the value of this method, a major drawback of this method is that no basic knowledge is collected on the cause of efficiency differences and the predictive value of the results is limited.

Acquisition of kinetic data requires more complicated procedures [5-7] than for collection of kinematics data, but it would provide a better understanding of pathological mechanism [8-11]. Tools for kinetic analysis of manual wheelchair propulsion analogous to the force platform system for gait, has developed in recently.[5-7]. A net joint moment represents the internal response of body segment to an external load. A net joint power can be calculated and used to document the net energy absorption or generation of the muscles [12]. However, the calculation of net moment and net power alone are insufficient to gain more insight into the energy expenditure. Also they could not show where the mechanical energy generated by muscles goes, where the energy absorbed by muscles comes from or where energy is transferred between segments. The total mechanical energy of a segment is the sum of its potential and kinetic energies. Complex movements, such as walking, often lead to the calculation of segmental kinematics from which mechanical energies are

derived[13-15]. This is a good method to describe the and qualifying human movements but it could not give any information about which muscle groups control this movement or how much they contribute to the segment' s motions. When the rate of change of total mechanical energy of a segment, also called mechanical power, is positive it means the energy level of this segment is increasing. Relative high correlation between work done by mechanical power and metabolic cost were found in past walking study[16-18]. The mechanical energy model was investigated in human walking for the evaluation of locomotion disorders [13-15], but not in wheelchair propulsion.

From mechanical point of view, the body energy can be calculated from kinematic and kinetic data by the power flow analysis approach. The change of mechanical energy for a given segment could be attributed to specific factors by power flow analysis. Those are joint power, in which energy is transferred between segments through the joint center and muscle power, in which muscle group generate, absorb or transfer energy[12, 19]. The characteristics of energy generation, absorption and transfer by muscles and energy transfer through the joints could be computed by combination of joint reaction forces and moments with segmental and joint kinematics. Some literatures applied it for gait analysis and validate it by comparing it with the rate of mechanical energy [12, 19]. To our knowledge, this mechanical model in analyzing mechanical inefficiency in wheelchair propulsion has not been available in literature. Without the knowledge of energetics, we would know nothing about the energy flows that cause the movement we are observing; and now movement would take place without those flows. Valid mechanical energy calculation is important for the investigation of mechanical efficiency when it is defined as the ratio of mechanical work (both internal and external) to metabolic

expenditure [12]. However, if the efficiency is defined as the ratio of external mechanical work to metabolic expenditure, the mechanical energy calculation also can help on understanding how the external work is produced.

Despite the high incidence of upper extremity musculoskeletal problems among individuals relying on wheelchairs, no studies have taken into account the mechanical energy and power flow of the musculoskeletal system for wheelchair propulsion. Mechanical energy and power flow have been a good tool for evaluation of locomotion disorders, such as walking in cerebral palsy children [14, 18]. The purpose of this study was to investigate the mechanical energy and power flow of the upper limb during wheelchair propulsion. Theoretically, the calculation of the rate of change of segmental total mechanical energy is equal to the sum of the segmental muscle and joint power. However, errors in the modeling of human form and experimental error in the measuring equipment could produce the discrepancies [19]. We will compare the total power flow with the segmental rates of change of mechanical energy to see the extent of the difference between. Furthermore the cause of energy of upper extremity will be discussed with focus on the role of energy transfer through muscles and joints.

Methods

Twelve young normal male adults (mean age 23.5 years old) were recruited for this study. None was reported any previous disorders and existed pains of upper extremity. The Hi-Res Expert Vision system (Motion Analysis Corp., Santa Rosa, CA, USA) was used to record the trajectories of the markers at 60 Hz. A set of fifteen reflective markers was placed on selected anatomic landmarks unilaterally on each subject. The selected anatomic

landmarks are as follows: processus xiphoideus, sternal notch, spinous process of the 7th cervical vertebra, acromion process, medial and lateral epicondyles of the elbow, radial and ulnar styloid processes, 3rd metacarpal, knuckle II and knuckle V. In addition, a triangular frame with three-markers was placed on the upper arm. An instrumented wheel system for three-dimensional kinetic analysis of upper extremity in wheelchair propulsion has been designed and validated [7, 20]. This system allows the direct measurements of three-dimensional dynamic forces and moments on the handrim during wheelchair propulsion in a laboratory setting as well as in the field. The instrumented wheel consists of a six-component load cell, a hand rim unit, a wheel, and a datalogger. The data logger and the Vision system were used synchronized to collect the data from subjects during wheelchair propulsion. Each subject had to propel at least five repetitions of wheelchair. A total of 60 propulsion trials were calculated.

The upper extremity is treated as a three segments linkage system. The three segments consist of the upper arm, forearm, and hand. Each of these three segments is treated as a rigid body. The marker's position was used to define the coordinate system, the center of gravity of each segment and the joint centers between segments. The trajectory data of the markers were smoothed using a generalized cross-validation spline smoothing routine (GCVAPL) at a cutoff frequency of 6 Hz. The hand is defined as a single rigid body connecting the mid-point between two markers on the knuckle II and knuckle V, and the mid-point between two

markers on the radial and ulnar styloid processes (center of the wrist joint). The forearm is defined as a single rigid body connecting the center of the wrist and the mid-point between the two markers on the medial and lateral epicondyles (center of the elbow joint). The upper arm is defined as a single rigid body connecting the center of the elbow and the marker on the acromion process. The positions of acromion process, medial epicondyle, and lateral epicondyle during wheelchair propulsion are calibrated using the local vectors with respect to the triangular frame on the upper arm in an anatomical neutral posture. This is done in order to avoid error resulting from skin movement.

The relative mass and relative location of the center of gravity of each segment will be determined using the segmental inertial data of Hinrichs (1990) and Yeadon (1989)[21, 22]. Angular velocity of each segment was determined by the Euler parameters. And the translation velocity of the joint center was calculated by the ratio of instant position change relative to the time interval. The dynamic force and moment on the handrim was used to determine the kinetics (joint force and moment) of upper extremity by inverse dynamic method. The moment of inertia about the three principal axes of each segment will be determined using the segment inertia data of Whitsett (1963)[23]. All the segment inertia data will be corrected to body weight and standing height [24]. All included vector in the calculation of mechanical energy and power flow using global coordinate system as reference. The Global coordinate system defined the x-axis points in the direction of wheelchair motion,

the y-axis points toward the subject' s left, and the z-axis is orthogonal to both the x- and y-axes.

Segmental Mechanical Energy Model

Kinetic energy ($\boldsymbol{E}_k$): The energy level of a body caused by its motion is called kinetic energy $\boldsymbol{E}_k$ and is calculated by the equation

$$\boldsymbol{E}_k = 1/2\ mv^2 + 1/2(I_{x'}\ \boldsymbol{\omega}_{x'}^2 + I_{y'}\ \boldsymbol{\omega}_{y'}^2 + I_{y'}\ \boldsymbol{\omega}_{y'}^2),$$

where m is mass; $v = \sqrt{v_x^2 + v_y^2 + v_z^2}$ is magnitude of the translational velocity of the center gravity of the body; I is the moments of inertia corresponding to the principal inertia axes of the body (x', y', z') with the components of the body' s rotational velocity along those axes used; and *?* is angular velocity of the body. Magnitude of the velocity is derived from all three components of the body's velocity in space (v_x, v_y, v_z). Thus, all components of the velocity of the body contribute to the kinetic energy of the body.

Potential energy ($\boldsymbol{E}_p$): The potential energy is calculated by the rise of body (h)× gravitational force:

$$\boldsymbol{E}_p = mgh$$

The *total mechanical energy* (E_i) of a segment i is the sum of its potential and kinetic energies.

$$\boldsymbol{E} = \boldsymbol{E}_p + \boldsymbol{E}_k$$

Power Flow Model

The power requirements of the segments discussed above are derived from the segmental mechanical energy calculations. These requirements can be compared with the power input to and transferred from the joints as calculated from the resultant joint loads and

the segmental velocities.

The joint power ($\boldsymbol{P}_j$) is equal to the vector dot product of the net joint force ($\boldsymbol{F}$) and the joint translational velocity ($\boldsymbol{V}$). The muscle power ($\boldsymbol{P}_m$) is the net joint moment ($\boldsymbol{M}$) dotted with the segmental angular velocity ($\boldsymbol{\omega}$)(not the joint rotational velocity) (Figure1a). Note that the forces and moments must be expressed in the same coordinate system as the segment velocity. The power flow of a segment was composed by the proximal/distal joint power ($\boldsymbol{P}_{jp}$ *and* $\boldsymbol{P}_{jd}$, distal denoted $_d$, proximal $_p$) and proximal/distal muscle power ($\boldsymbol{P}_{mp}$ *and* $\boldsymbol{P}_{md}$) (Figure1b).The total power flow applied to or taken from the body is the summation of the joint power and muscle power at each end. For a typical segment, the equation expressing this joint, muscle and total power is

$$\boldsymbol{P}_j = \boldsymbol{F} \bullet \boldsymbol{V}$$

$$\boldsymbol{P}_m = M_p \bullet \boldsymbol{\omega}$$

$$\boldsymbol{P}_f = \boldsymbol{P}_{jp} + \boldsymbol{P}_{mp} + \boldsymbol{P}_{jd} + \boldsymbol{P}_{md} = \boldsymbol{F}_p \bullet \boldsymbol{V}_p + M_p \bullet \boldsymbol{\omega} + \boldsymbol{F}_d \bullet \boldsymbol{V}_d + \boldsymbol{M}_d \bullet \boldsymbol{\omega}$$

Subscript $_d$ and $_p$ meant the distal and proximal part of segment respectively.

Variables were normalized to 100% cycle. Each propulsion cycle include propulsion and recovery phases. The mechanical energy and power flow parameters were averaged for these five trial repetitions to represent the subject performance. Also, these average variables of each subject were averaged again to represent the ensemble performance. For comparing the difference between total power flow with the segmental rates of change of mechanical energy, cross correlation analysis was used to determine the similarity of two such sets of series values [25-27]. Cross correlation analysis could help to determine the amplitude similarity the two set of data represented by the peak coefficient (r) and to examine if there was a time lag between the two set of data by the normalized cycle (% cycle) shift. For perfectly

symmetry, the *r*-value would be 1 and the percent GC shift would be 0.

Results

Stick diagram representation of upper extremity for wheelchair propulsion was showed in Figure 2 with 0.05 sec interval. The upper extremity segments moved downward during propulsion phase and upward during recovery phase.

The total mechanical energy was composed by the potential and kinetic energy (Figure 3). Ground level was assumed to be the zero potential energy such that the total energy was larger for the upper arm than the forearm and hand. These three segments had different pattern during propulsion cycle. For the hand segment, it increased during initial propulsion and reached the peak at earlier propulsion phase than the forearm and upper arm did. After then, the total mechanical energy decreased to the smallest value at initial recovery and then increased again till the end of recovery phase. The total energy change was 1.0 J for the hand, 2.3 J for the forearm and 1.3 J for the upper arm. The pattern of kinetic energy was different from the total mechanical energy, its magnitude decreased in the recovery phase and reached the smallest value. Potential energy began to decrease from initial propulsion and had the smallest magnitude at the end of propulsion phase. Three segments of the upper extremity had similar potential energy patterns but different kinetic energy patterns. The kinetic energy of the hand increased in initial propulsion and reached the peak at earlier propulsion phase than the forearm and upper arm segments did. The mechanical energy pattern showed a partial complement trend (i.e., when kinetic energy increased potential energy decreased over time and when kinetic energy decreased potential energy increased over time). For the hand segment, the complement trend was lost from the middle to the end of propulsion phase. During this period, both the potential and kinetic energy decreased.

Figure 4 showed the power of all segments. The patterns of power flow of each segment

were quite similar. They were positive before the mid-propulsion and changed to negative value since then. The maximum negative magnitude appeared at the end of propulsion phase and then the magnitude of power flow increased and changed to be positive after the mid-recovery phase. The forearm had the greater variation than the upper arm and hand. Figure 5 showed the components of power flow for the segment of the upper arm, forearm and hand during propulsion. The total power of a segment was composed by the proximal/distal joint power ($\boldsymbol{P}_j$) and proximal/distal muscle power ($\boldsymbol{P}_m$). The joint powers in adjacent segments always have a joint power equal in magnitude but opposite in sign. That because the adjacent segments connected at joint had the same velocity vectors but their forces is equal in magnitude and opposite in direction. Contrary to the situation for the joint power, the adjacent segments connected at joint do not necessary to have the same segmental angular velocity. Consequently, the power flow by muscle could be more complicated than by joint, which could only transfer energy. The muscle can also generate or absorb mechanical energy by concentrically or eccentrically contracting, respectively. The components of power flow showed that the upper arm had larger muscle power compared to the forearm and hand. Meanwhile, the joint power was larger than the muscle power. During propulsion phase, the proximal joint power was positive (i.e. the rate of energy influxes the segment) and distal one was negative (i.e. the rate of energy outflows the segment).

The rate of change of mechanical energy and power flow of the upper limb was shown in Figure 6. When the powers were positive, it meant the energy level of this segment is increasing. The rate of change of mechanical energy showed a similar pattern with power flow. The *r* value for the upper arm, forearm and hand is 0.84, 0.91, 0.92 respectively. And the time lag for the upper arm is 5%GC and 0 for both forearm and hand. The discrepancy between the rate of change of mechanical energy and power flow was smaller on the forearm and hand compared to the upper arm. The absolute value of power flow was always greater

than that of the rate of change of mechanical energy.

Discussion

From the components of mechanical energy of these three segments, we know that the kinetic energy, especially the translational kinetic energy, was the source for increased total mechanical energy during propulsion phase. However, during recovery phase the total mechanical energy was increased by potential energy. The internal work done by the musculoskeletal system is to move the segments of upper extremity during propulsion phase, while it is used to elevate the segments during recovery phase. During propulsion phase, the variation in kinetic energy pattern between these three segments results in the dissimilarity of total mechanical energy pattern. The variations in kinetic energy pattern result from the different movement speeds among three upper limb segments, the fast on the hand first, then forearm and the slowest on the upper arm. The proximal part of upper extremity acts as an actuator and stabilizer to move the wheel forward during early propulsion phase.

The total mechanical energies of these three segments changed within a small range. The greatest change is found on the forearm and the least on the hand. The energy change could be further explicit by the power flow analysis. During recovery phase the total mechanical energy increased by potential energy, is supplied by the proximal joint power which is mainly from the trunk flexor (or gravity). At the same time, the trunk flexor (or gravity) act eccentrically to slow down the backward movement of the trunk. This joint power is transferred from the upper arm to forearm and hand. During propulsion phase, the increase of total mechanical energy is from both proximal muscular power and proximal joint power. However, the proximal joint power is from the trunk flexor (or gravity) and proximal muscular power is from the shoulder flexor. These two powers are integrated and transferred to the forearm and hand. Trunk flexor concentrically contracts to accelerate forward

movement. As the same event, the shoulder flexor acts concentrically to speed up the shoulder flexion movement and generate a net joint angular power at the shoulder.

For the upper arm, during the first two third of propulsion phase, the joint power flow is transferred downward to the forearm and hand (Figure 7). This power is transferred to the hand and used to propel the wheel forward. Throughout the whole propulsion phase, the distal joint power of hand was negative (outflow). This means, for the entire propulsion phase, the hand provides the energy to drive the wheel. Although the power flow pattern is quite complex, the purpose of upper extremity movement is quite clear. From the terminal propulsion to middle recovery phase, the joint power flow is transferred upward to trunk from the upper arm and forearm (Figure 7). This is to conserve the energy of upper extremity in trunk for next propulsion phase. During recovery phase, the upper arm has a proximal muscular power from the shoulder extensor. It acts concentrically to extend the shoulder.

Theoretically, the calculation of the rate of change of segmental total mechanical energy is equal to the sum of the segmental muscle and joint power. However, errors in the modeling of human form and experimental error in the measuring equipment could produce the discrepancies[12, 19]. That similar patterns exist between two different power calculations may reveal our energetic model may be reasonable. However, great discrepancy existed in the upper arm may result from its special characteristics, larger powers but less movement compared to the forearm and hand. A minor error in calculating the powers could lead a great difference in the rate of energy change [19].

Another possible reason was proposed by the difference of meaning of this two power calculations. The power requirements of the segments can be derived from the segmental mechanical energy calculations. These requirements can be compared with the power input to and transferred from the joints as calculated from the resultant joint loads and the segmental velocities. The muscles must maintain joint stability and propulsion while attempting to

minimize energy expenditure. Thus, it would be expected that the power supplied to segments is often greater than the mechanical requirements. The more discrepancy between these two powers estimates, there is much inefficiency in energy expenditure during wheelchair propulsion. These two powers estimate could lead to the calculation of the work by integration of the power curve with the time during wheelchair propulsion. The work was calculated from the absolute change of the sum of all segments powers, which allows transfers of energy within the segment and between adjacent segments of the same limb. This method was called WWB (work within the segment and between adjacent segments) method [17, 18], was proved to be a reliable indication of metabolic cost [18]. From the two power estimates in the current study, we used the WWB method to calculate the work done in per propulsion. The work per propulsion calculated from the rate of change of mechanical energy and power flow was 9.41 (SD, 2.39), 13.70 (SD, 3.54) individually. The work calculated by power flow is statistically significant larger than that calculated from the rate of change of mechanical energy ($p<0.05$) by ANOVA analysis. It could mean that the power supplied to segments is indeed greater than that required. We could use the difference between these two power estimates as an index to individualized guidelines for the configuration of handrim wheelchairs. The individualized guidelines will lead to an improvement of the efficiency of handrim wheelchair propulsion and a smaller risk of upper extremity complaints.

The limitation of this study is using the young normal male adults as subject that patient regularly using wheelchair may have different energy and power flows. Also, it is possible to have co-contraction of muscles in upper extremity during wheelchair propulsion and it is hard to distinguish by these methods. However, no literature reveal most wheelchair propulsion period is co-contraction for muscles in the upper extremity. The EMG study showed all muscles functioned either in push or recovery phase [28]. The shoulder agonist muscles (anterior deltoid/ pectoralis major) acted in push phase and the antagonist muscles (middle

and posterior deltoid) acted in recovery phase. It is similar performance for the biceps and triceps brachil on elbow.

The joint power play an important role for energy transfer as well as the muscle generate and absorbing energy between segments during wheelchair propulsion. The understanding of the mechanical energy and power flow in the upper limb is helpful to understand the mechanical efficiency of manual wheelchair propulsion.

Acknowledgments

This work was supported by the National Health Research Institute grant NHRI-EX90-9019EL and National Science Council grant NSC89-2614-E-242-001, TAIWAN.

References

[1] van der Woude LH, Veeger DJ, Rozendal RH, Sargeant TJ. Seat height in handrim wheelchair propulsion. J Rehabil Res Dev 1989;26:31-50.

[2] van der Woude LH, Veeger HE, Rozendal RH, van Ingen Schenau GJ, Rooth F, van Nierop P. Wheelchair racing: effects of rim diameter and speed on physiology and technique. Med Sci Sports Exerc 1988;20:492-500.

[3] Cooper RA, Horvath SM, Bedi JF, Drechsler-Parks DM, Williams RE. Maximal exercise response of paraplegic wheelchair road racers. Paraplegia 1992;30:573-81.

[4] Veeger HE, van der Woude LH, Rozendal RH. Effect of handrim velocity on mechanical efficiency in wheelchair propulsion. Med Sci Sports Exerc 1992;24:100-7.

[5] Asato KT, Cooper RA, Robertson RN, Ster JF. SMARTWheels: development and testing of a system for measuring manual wheelchair propulsion dynamics. IEEE Trans Biomed Eng 1993;40:1320-4.

[6] Cooper RA, Robertson RN, VanSickle DP, Boninger ML, Shimada SD. Methods for determining three-dimensional wheelchair pushrim forces and moments: a technical note. J Rehabil Res Dev 1997;34:162-70.

[7] Wu HW, Berglund LJ, Su FC, Yu B, Westreich A, Kim KJ et al. An instrumented wheel for kinetic analysis of wheelchair propulsion. J Biomech Eng 1998;120:533-5.

[8] Robertson RN, Boninger ML, Cooper RA, Shimada SD. Pushrim forces and joint kinetics during wheelchair propulsion. Arch Phys Med Rehabil 1996;77:856-64.

[9] Boninger ML, Cooper RA, Robertson RN, Shimada SD. Three-dimensional pushrim forces during two speeds of wheelchair propulsion. Am J Phys Med Rehabil 1997;76:420-6.

[10] Kulig K, Rao SS, Mulroy SJ, Newsam CJ, Gronley JK, Bontrager EL et al. Shoulder joint kinetics during the push phase of wheelchair propulsion. Clin Orthop 1998:132-43.

[11] Boninger ML, Cooper RA, Baldwin MA, Shimada SD, Koontz A. Wheelchair pushrim

kinetics: body weight and median nerve function. Arch Phys Med Rehabil 1999;80:910-5.

[12] Winter DA. Biomechanics and motor control of human movement. New York: John Wiley & Sons; 1994.

[13] Winter DA. A new definition of mechanical work done in human movement. J Appl Physiol 1979;46:79-83.

[14] Olney SJ, Costigan PA, Hedden DM. Mechanical energy patterns in gait of cerebral palsied children with hemiplegia. Phys Ther 1987;67:1348-54.

[15] Winter DA. Energy generation and absorption at the ankle and knee during fast, natural, and slow cadences. Clin Orthop 1983:147-54.

[16] Burdett RG, Skrinar GS, Simon SR. Comparison of mechanical work and metabolic energy consumption during normal gait. J Orthop Res 1983;1:63-72.

[17] Frost G, Dowling J, Baror O, Dyson K. Ability of mechanical power estimations to explain differences in metabolic cost of walking and running among children. Gait Posture 1997;5:120-7.

[18] Unnithan VB, Dowling JJ, Frost G, Baror O. Role of mechanical power estimates in the O-2 cost of walking in children with cerebral-palsy. Med Sci Sports Exerc 1999;31:1703-8.

[19] Gordon D, Robertson E, Winter DA. Mechanical energy generation, absorption and transfer amongst segments during walking. J Biomech 1980;13:845-54.

[20] Wu HW, Su FC, Berglund L, Chang YW, An KN. Development and Testing of a System for Measuring Manual Wheelchair Propulsion Dynamics. Chinese Journal of Medical and Biological Engineering 1996;16:244-56.

[21] Hinrichs RN. Adjustments to the segment center of mass proportions of Clauser et al. (1969). Journal of Biomechanics 1990;23:949-51.

[22] Yeadon MR, ., Morlock M. The appropriate use of regression equations for the estimation of segmental inertia parameters. . Journal of Biomechanics 1989;22:683-9.

[23] Whitsett CE. Some dynamic response characteristics of weightless man. OH: Wright-Patterson Air Force Base; 1963.

[24] Dapena J. A method to determine the angular momentum of a human body about three orthogonal axes passing through its center of gravity. Journal of Biomechanics 1978;11:251-6.

[25] Sadeghi H, Allard P, Prince F, Labelle H. Symmetry and limb dominance in able-bodied gait: a review. Gait Posture 2000;12:34-45.

[26] Hannah RE, Morrison JB, Chapman AE. Kinematic symmetry of the lower limbs. Arch Phys Med Rehabil 1984;65:155-8.

[27] Arsenault AB, Winter DA, Marteniuk RG. Bilateralism of EMG profiles in human locomotion. Am J Phys Med 1986;65:1-16.

[28] Mulroy SJ, Gronley JK, Newsam CJ, Perry J. Electromyographic activity of shoulder muscles during wheelchair propulsion by paraplegic persons. Arch Phys Med Rehabil 1996;77:187-93.

Figure Legends

Figure 1: (a) Variables included in the calculation of the joint power ($\boldsymbol{P}_j$) and muscle power ($\boldsymbol{P}_m$) for a rigid body, $\boldsymbol{P}_j = \boldsymbol{F} \bullet \boldsymbol{V}$, $\boldsymbol{P}_m = M_p \bullet \boldsymbol{\omega}$. (b) Total power flow ($\boldsymbol{P}_f$) is composed by the summation of the joint and muscle power at proximal and distal ends (Subscript $_p$ and $_d$ meant the proximal and distal part of segment respectively). $\boldsymbol{P}_f = \boldsymbol{P}_{jp} + \boldsymbol{P}_{mp} + \boldsymbol{P}_{jd} + \boldsymbol{P}_{md}$

Figure 2: Stick diagram representation of upper extremity for wheelchair propulsion with 0.05 sec interval during propulsion phase (a) and recovery phase (b)

Figure 3: Mean mechanical energy of the upper arm (a), forearm (b) and hand (c)

Figure 4: Mean power flow of the upper limb segments

Figure 5: Components of mean power flow of the upper arm (a), forearm (b) and hand (c)

Figure 6: Power flow and the rate of change of mechanical energy of the upper arm (a), forearm (b) and hand (c)

Figure 7: Illustration figure to show the power flow in upper extremity during initial propulsion phase (a) and terminal propulsion phase (b)

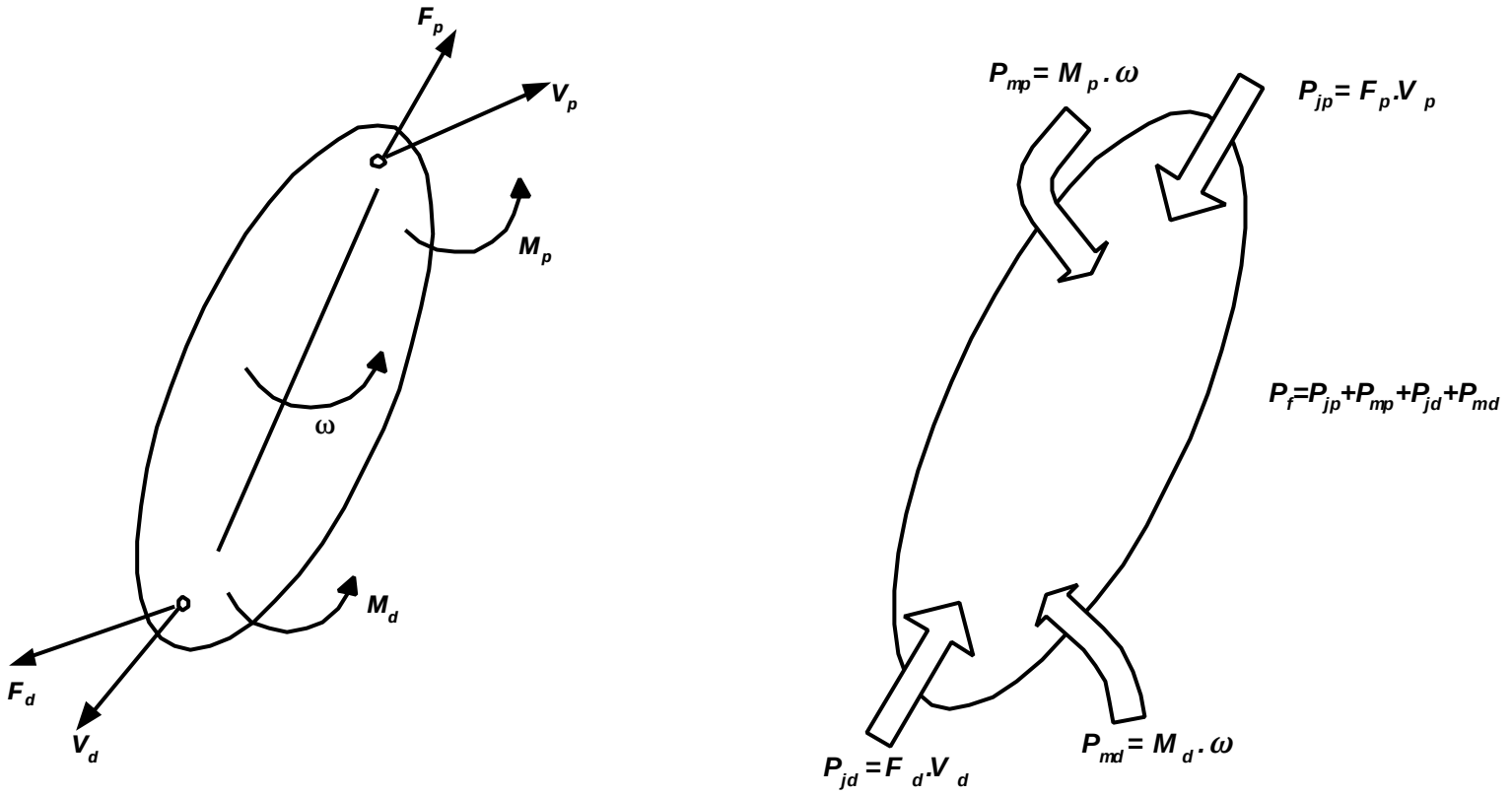

Figure 1: (a) Variables included in the calculation of the joint power $(\boldsymbol{P}_j)$ and muscle power $(\boldsymbol{P}_m)$ for a rigid body, $\boldsymbol{P}_j = \boldsymbol{F} \bullet \boldsymbol{V}$, $\boldsymbol{P}_m = M_p \bullet \boldsymbol{\omega}$ (b) Total power flow $(\boldsymbol{P}_f)$ is composed by the summation of the joint and muscle power at proximal and distal ends (Subscript $_p$ and $_d$ meant the proximal and distal part of segment respectively). $\boldsymbol{P}_f = \boldsymbol{P}_{jp} + \boldsymbol{P}_{mp} + \boldsymbol{P}_{jd} + \boldsymbol{P}_{md}$

(a)

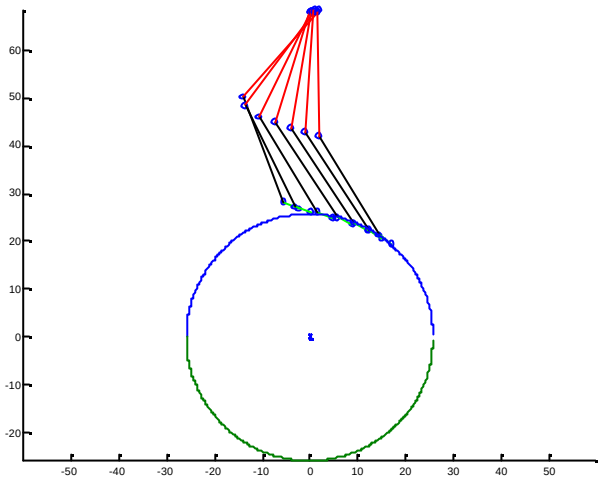

(b)

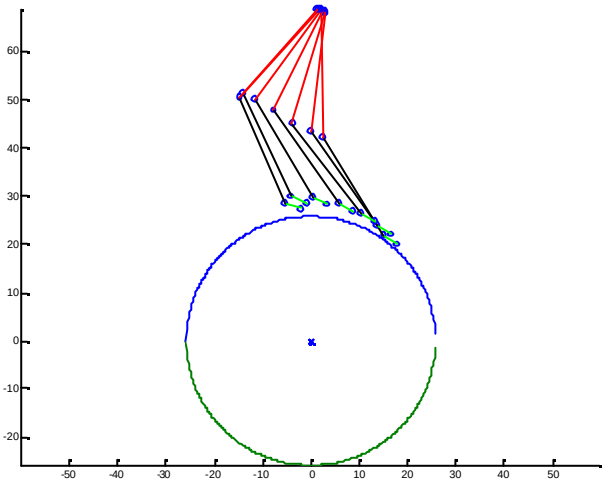

Figure 2: Stick diagram representation of upper extremity for wheelchair propulsion with 0.05 sec interval during propulsion phase (a) and recovery phase (b)

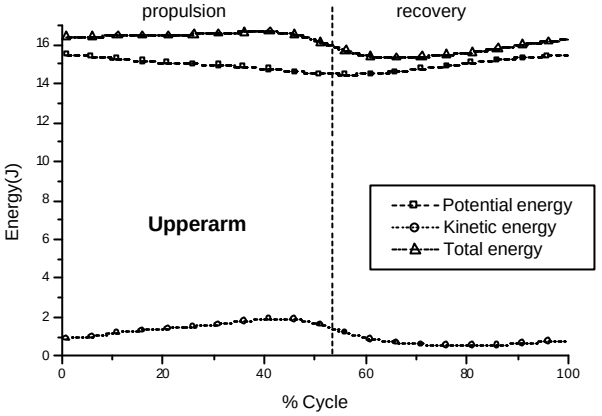

(a)

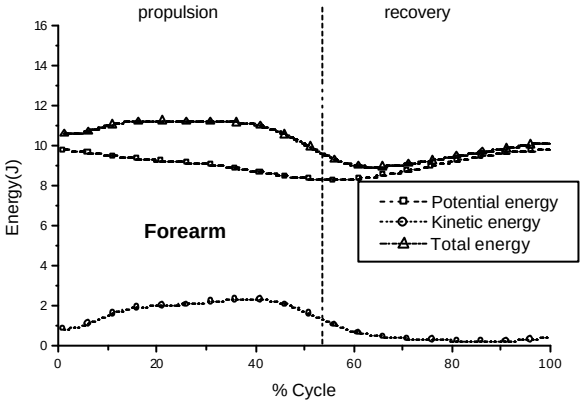

(b)

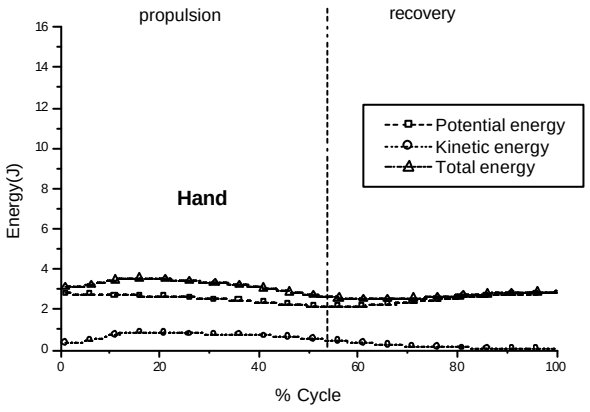

(c)

Figure 3: Mean mechanical energy of the upper arm (a), forearm (b) and hand (c)

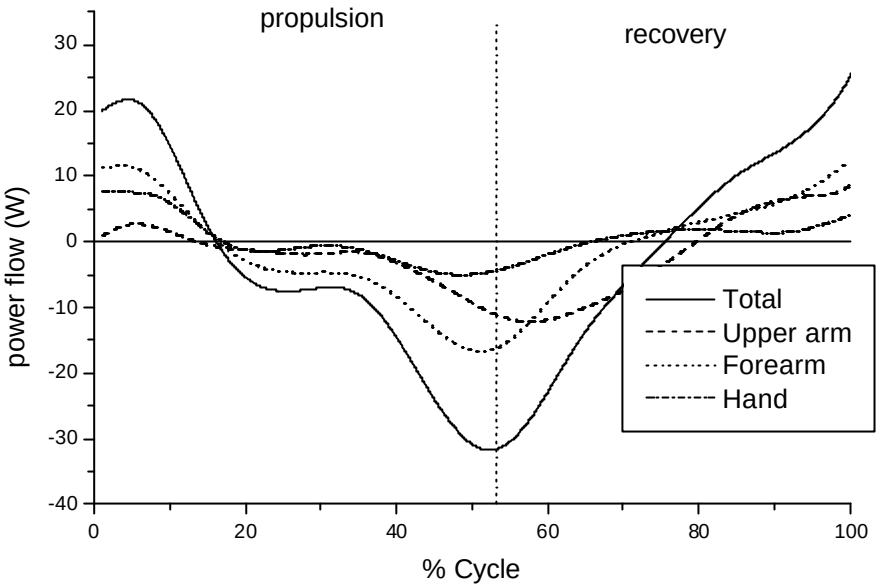

Figure 4: Mean power flow of the upper limb segments

(a)

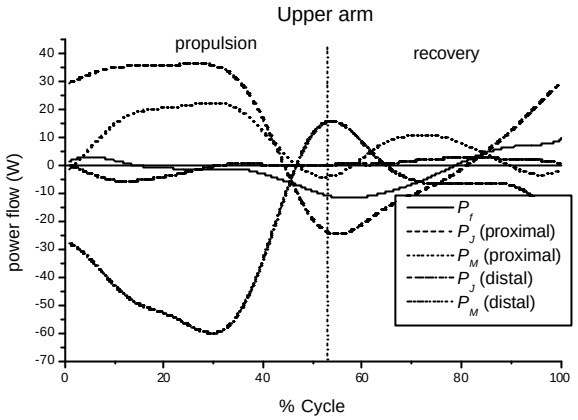

(b)

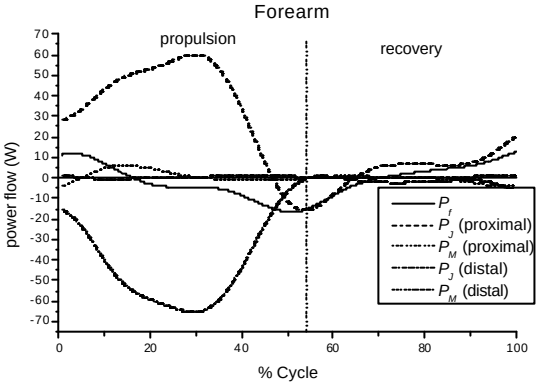

(c)

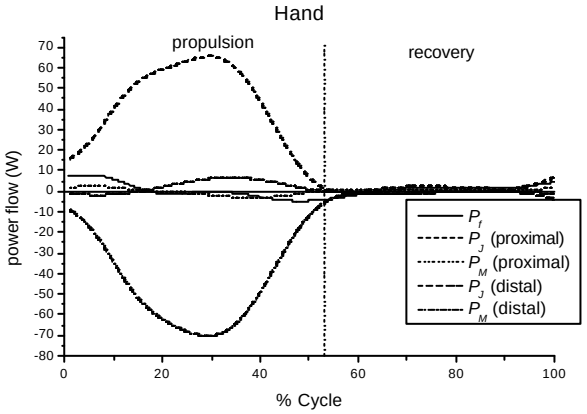

Figure 5: Components of mean power flow of the upper arm (a), forearm (b) and hand (c)

(a)

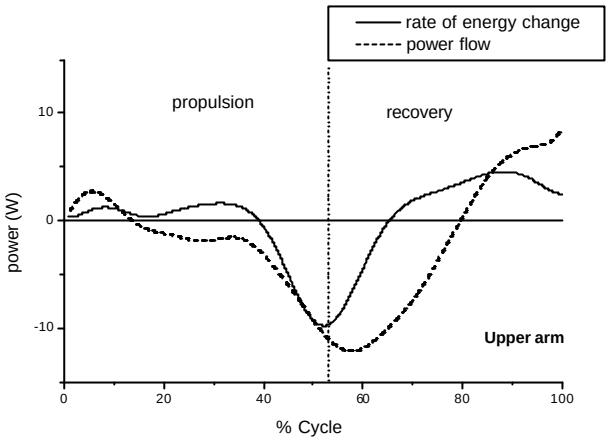

(b)

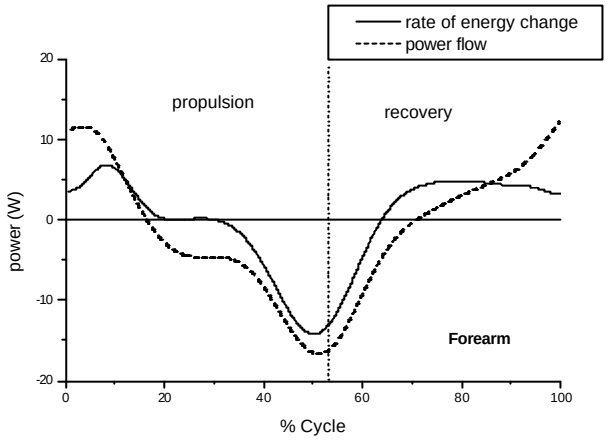

(c)

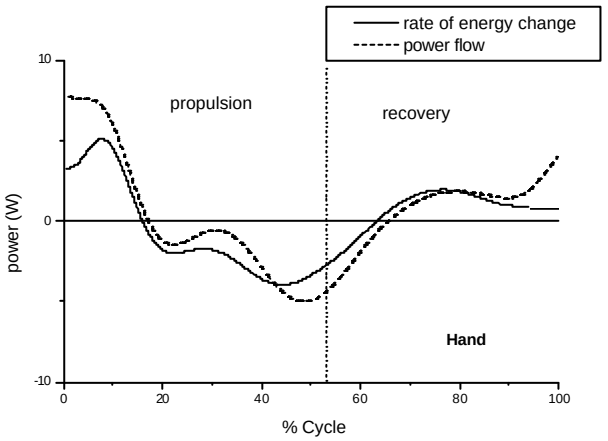

Figure 6: Power flow and the rate of change of mechanical energy of the upper arm (a), forearm (b) and hand (c)

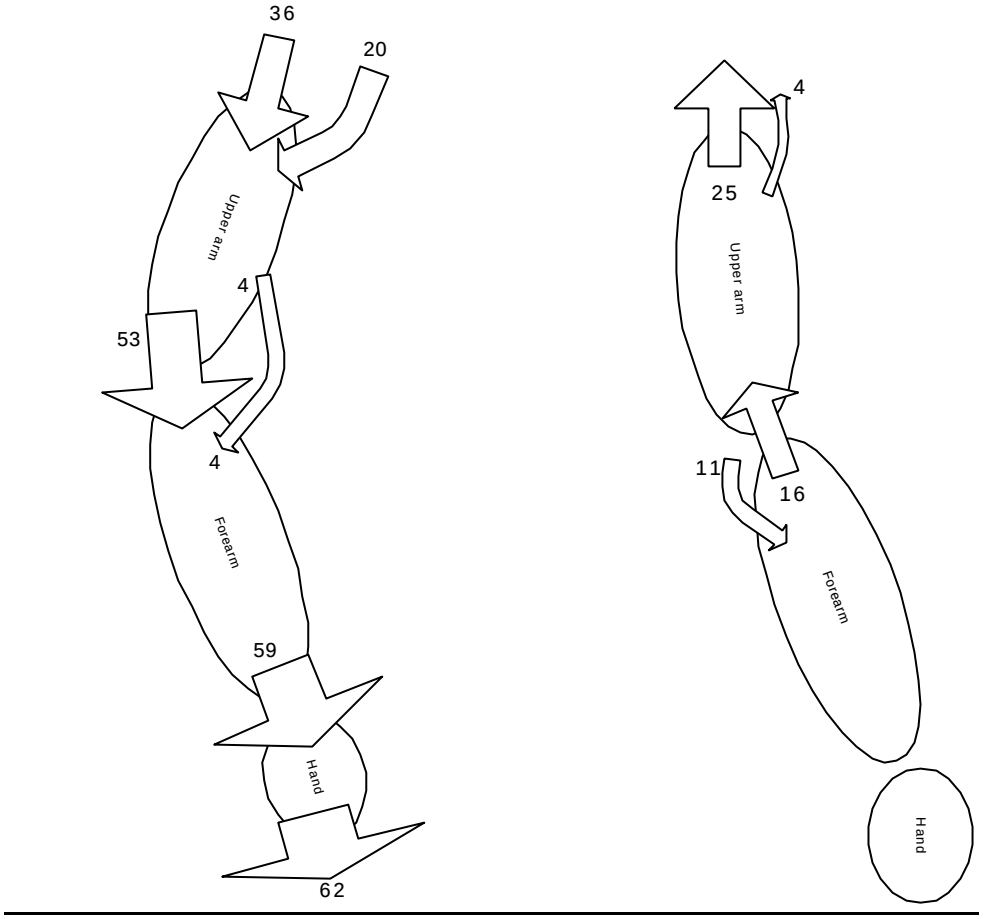

Figure 7: Illustration figure to show the power flow in upper extremity during initial propulsion phase (a) and terminal propulsion phase (b), the straight arrow representing joint power and curve arrow representing muscle power.

Modeling of Manual Wheelchair Propulsion Using Optimization Method

LY Guo, KD Zhao, FC Su*, and K-N An, Ph.D.**

Orthopedic Biomechanics Laboratory
Mayo Clinic
Rochester, MN 55905

***Institute of Biomedical Engineering**
National Cheng Kung University
Tainan, 701 TAIWAN

***Corresponding Author:**
Kai-Nan An, Ph.D.
Mayo Clinic
200 First Street SW
Rochester, MN 55905
Phone: 507-538-1717
Fax: 507-284-5392
Email: an.kainan@mayo.edu

ABSTRACT

Collection of biomechanical data is essential for understanding handrim wheelchair propulsion. Biomechanical models can add to our understanding by clarifying how upper extremity segments and muscles interact to execute the motor task. Therefore, we have developed a two-dimensional model of the upper arm, forearm, and wheelchair wheel to study different aspects of the man-machine environment, including the mechanical constraints and effectiveness of force application while propelling a wheelchair. The goal of this study is to develop and validate the model as well as present predictions of handrim kinetics during wheelchair propulsion.

A planar model was developed at incremental changes in wheel angle throughout the propulsion cycle. Anthropometric and strength data were collected from subjects as inputs to the model and model predictions of handrim force and progression moment were compared to those collected from the subjects during quasi-static wheelchair propulsion.

The model predicted a progression moment that is larger at the initial and terminal propulsion positions (i.e. wheel angles of 120 and 60 degrees respectively) and is smaller in mid-propulsion. The experimental results supported this finding. This phenomenon may result from a mechanical disadvantage of the upper arm musculature at mid-propulsion. At mid-propulsion, the reaction force on the hand is nearly perpendicular to the moment arms of the force about the shoulder and elbow. Thus, even small forces result in large moments at the two joints. Differences in force direction are quite small between model and experiment at all propulsion positions.

Differences in force magnitude and progression moment between model and experiment were smaller in the initial and mid propulsion hand positions than in the terminal propulsion.

A planar model has been successfully developed and validated which could be useful in examining the mechanics of wheelchair propulsion and in wheelchair design and fitting. In the future, the model will be further refined to include muscle dynamics and to be three-dimensional.

Key Words: Wheelchair; Biomechanics; Optimization, Model

Introduction

Wheelchair design affects the performance of propelling a wheelchair. The relationship between handrim wheelchair design and performance has been studied for the effect of features such as seat height[1-3], fore-aft position[2, 3] and handrim diameter[4]. Variability in the propulsion technique in manual wheelchair users due to differences in level of injury and wheelchair fit makes detection of subtle changes in technique nearly impossible. However, such changes are well suited to analytical modeling techniques, since variables can be manipulated systematically and the effects of the manipulation can be easily quantified.

van der Helm et al.(1996) used a developed musculoskeletal model to simulate muscle force in the shoulder during wheelchair propulsion[5]. They collected statically applied handrim forces in five hand positions and five different load levels per hand positions. Upper extremity position and measured handrim forces were input to an inverse dynamic model which output muscle forces subject to an optimization criterion. The criterion used was minimization of the sum of squared muscle stresses. The largest external moments for the hand were found in the top dead center position on the handrim. This result was in contrast to that found during dynamic propulsion. In addition, the force direction during static wheelchair propulsion was more tangential to the handrim than during dynamic wheelchair propulsion.

Rozendaal and Veeger (2000) simulated the hand rim force direction based on experimental data from wheelchair users [6]. They suggested that a force generated tangential to the handrim could have greater mechanical effect on wheel progression, while a force more perpendicular to the line from hand to elbow or the line from hand to the shoulder will have a large musculosketetal cost on the muscles of these two joints. They used a ratio of mechanical effect and musculoskeletal cost in wheelchair propulsion as an optimization criteria in their simulations to find the applied force direction. The direction of the simulated force data during the middle and terminal parts of propulsion are comparable to the actual force measured by experiment. However, the force direction during initial propulsion was directed away from the wheelhub differing from the inwardly directed pattern during real wheelchair propulsion. Also, the maximum effect-cost ratio obtained in initial propulsion was smaller than at the end of propulsion, means at the terminal propulsion phase is a appropriate position for generate larger force on the handrim. This differed from the results of dynamic wheelchair propulsion, when the greatest applied force appeared in middle propulsion.

Collection of biomechanical data is essential for understanding handrim wheelchair propulsion. However, biomechanical models can add to our understanding of how upper extremity segments and muscles interact to execute the motor task [7].

Through modeling, different aspects of the man-machine-environment can be investigated includingthe mechanical constraints of force application . In addition, ineffective force generation can be investigated as well as the inadequacy of wheelchair pushing techniques[8, 9].Therefore, we have developed and validated a model of the upper arm, forearm, and wheelchair wheel to study changes in the wheelchair-user interface.

Research Design and Methods

Five healthy male subjects, mean age 35.2 years old, participated in this study. Anthropometric measurements were collected from all subjects , including the length of upper arm and forearm as well as the shoulder position related to the wheel axle (list all variables here) as shown in Table 1. The point of force application on the handrim was assumed to be the second metacarpophalangeal (MCP) joint, as has been assumed by several other investigators [10, 11] so the forearm length was measured from the lateral epicondyle to the 2nd MCP. The length of the upper arm was measured from the acromion to lateral epicondyle.

The kinematics data of upper extremity will be further determined by the four-bar linkage model mentioned above to simulate the upper extremity movement during different hand position. Using a Kincom125 AP® dynamometer, the isometric shoulder flexion and extension muscle strengths were measured at 20 and 40 degrees of shoulder and 0, 20, 40, 60, 80.degrees of shoulder flexion with the elbow at 90 degrees and the forearm in the neutral position. The isometric elbow flexion and

extension strengths were measured at 0, 20, 40, 60, 80, 100.and 120 degrees of elbow flexion with the forearm in the neutral position. Muscle strengths at each specific position were determined as the peak force generated during a three second contraction. At each specific position, three trials of muscle strength data were collected allowing enough time between trials for the muscle to rest to avoid muscle fatigue. All the measured forces were input into a regression model to obtain the best second order polynominal fit for the data. This curve, together with the kinematics of the upper extremity, as determined by a four-bar linkage model, was used to find the allowable limits of muscle strength.

The optimization model

The rationale for the model is, given a subject-specific profile of the strengths of each of the upper extremity joints as a function of joint angle, there is an optimal direction of force application to the handrim to maximize the propulsion moment about the wheel axle at each instant throughout the propulsion cycle. This optimal direction can be determined at each instant by formulating a linear optimization problem which aims to maximize the moment about the wheel axle (M_o) subject to the constraints of the subject' s shoulder and elbow joint moment-generating capabilities for the joint angles specified. The formulation is as follows (Figure1):

Maximize M_o

Subject to:

$M_s = P_s \times F_h$

$M_e = P_e \times F_h$

$M_o = P_r \times F_h$

$-M_{se} \leq M_s \leq M_{sf}$

$-M_{ee} \leq M_e \leq M_{ef}$

where the unknown independent variable, F_h, is the force vector applied by the hand on the handrim; M_s and the M_e are the flexion/extension moments at the shoulder and elbow joints, respectively, due to the force F_h at the handrim; F_h at the handrim; M_r is the moment about the wheel axle generated by the force F_h at the handrim; P_s, P_e, and P_r are the position vectors of the shoulder, elbow, and wheel axle relative to the point of force application on the handrim. M_{se} and M_{sf} were the maximum shoulder joint strengths in extension and flexion, respectively; M_{ee} and M_{ef} were the maximum elbow joint strengths in extension and flexion, respectively. The optimization was performed using the Matlab Optimization Toolbox (The Mathworks, Inc.).

Modeling Verification

An instrumented wheel system was used to measure directly three- dimensional dynamic forces and moments on the handrim during wheelchair propulsion. However, only the applied forces in the laboratory reference frame (x and y axes) and progression moments around the wheel axle were recorded for use in this planar model. The wheelchair had a handrim size of 25.4 cm and was locked to prevent forward movement as the subjects propeled the handrim with maximum effort. Five hand positions corresponding to a wheel angle of 120, 105, 90, 75 and 60 degreeswere assigned to the subject in a random order. The five subjects performed four trials of maximal wheelchair propulsion effort for each hand position. Each variable (what variables?) was averaged for these four repetitions to represent the subject's

performance for a given hand position. The force direction and magnitude of force applied to the handrim were determined and compared to the results calculated from the model.

Results

Isometric muscle strengths of the shoulder and elbow showed a typical pattern among the five subjects. Shoulder flexion decreased as the shoulder flexion angle increased (Figure 2a). In contrast, the shoulder extensor strength increased as shoulder flexion angle increased to a maximum value of 80 degrees. The elbow flexor and extensor strength curves for all subjects showed an ascending and descending trend, with peak flexion occurring at 60 degrees of flexion and peak extension torque occuring at 80 degrees of flexion (Figure 2b). The second order polynominal regression model significantly predicted the muscle strength from value of joint angle for all subjects and all muscle groups ($P<0.05$).

The quasi-static model predicted that the shoulder went from a position of extension to greater extension initially then reversed direction into flexion. During the initial propulsion phase, it went from a flexion position into greater flexion. At approximately the midpoint of propulsion the elbow began to extend until the end of the stroke. As shown in Table 2, the results of the model revealed the progression moment was greater at both initial and terminal propulsion positions (i.e. wheel angles of 120 and 60 degrees respectively) and was smaller in the mid-propulsion position (i.e. wheel angle of 90 degrees). The experimental results supported this finding (Table 2 and Figure 3). The difference in progression moments between model and

experiment was small in initial and mid-propulsion hand positions but greater in the terminal propulsion positions. The directions of applied force applied to the handrim by both experiment and model in the different hand positions were similar (Figure 4a and 4b). They were upward before the hand passed the top dead center and were downward after the hand passed the top dead center. The differences in force direction between model and experiment ranged from 2.6 to –28.2 degrees (Table 2). The difference in force magnitude between model and experiment had a similar trend to the results of progression moment, with smaller differences seen in initial and mid propulsion hand positions but greater differences seen in terminal propulsion positions (Table 2).

Discussion

The current study results reveal the disadvantage propulsion design of a standard handrim wheelchair. During dynamic wheelchair propulsion, the progression moment reaches its maximum value in mid-propulsion phase as required by the biomechanics of the movement. However, our model reveals that the hand position in mid-propulsion is not optimal for the upper extremity to generate a large force on the handrim. Because this force is nearly perpendicular to the line from the hand to shoulder will result in a large shoulder moment. Similarly, the applied propulsion force also acts nearly perpendicular to the line from hand to elbow which could require a large elbow moment [5, 6]. In terminal propulsion, the applied force acts is

more in line with the line from hand to shoulder as well as with the line from hand to elbow resulting in the ability of the upper extremity to generate larger forces and progression moments. The model has helped to provide insight into the potential maximum moment generating capacity of a user given a specific configuration of the wheelchair. In addition we can consider if the handrim wheel design could be altered to allow the user to propel the handrim with a greaterprogression moment. For example, in wheelchair racing, users always flex their trunk anteriorly to propel the handrim with hand anterior to top dead center. This hand position allows larger progression moments to be generated because their lever arms enable the upper extremity to tolerate greater external loading.

During propulsion, almost 50% of the forces exerted at the pushrim are not directed toward forward motion and, therefore, either apply friction to the pushrim or are wasted. However, some investigators do not agree with the concept that non-tangentially directed forces arewaste or just misdirected [12]. To apply a push force in the mechanically most optimal direction, tangential to the rim, a contradictory situation occurs in which the elbow joint is extending. A flexor moment ought to be generated for mechanically optimal results. This situation will lead to production of negative power, and hence, be ineffective regarding co-ordination and physiology. Our results support this concept, the optimized force direction is not purely tangential

to the handrim and passes through the upper arm segment. Optimized force direction is acquired as both the shoulder flexors and elbow extensors reach their physical constraints. If the optimized force direction is tangential to the handrim, the shoulder flexor will reach its constraint and a smaller wheel progression moment will be generated.

This current study is like several static maximum isometric contractions on different handrim positions. The results show the force vector is roughly tangential to the handrim. The force vector is upward when the hand position is posterior to top dead center and it is downward when the hand position is anterior to top dead center. These predictions agree with the dynamic wheelchair propulsion experimental data collected by van der Helm (1996)[5]. However, the force direction posterior to the top dead center of the handrim differed greatly from the experiment results of the dynamic wheelchair propulsion. The direction of handrim force during dynamic wheelchair propulsion is always downward during the whole propulsion phase including the period when the hand position is behind top dead center [13-15]. For the push force to be upward, the elbow flexor must be activated. But halfway through the propulsion phase the applied force must change to progress the wheel so the elbow extensor needs to be activated. The change in muscle activation from elbow flexor to elbow extensor will result in more complex and inneficient movement [12, 16, 17].

However, during modeling ofstatic propulsion, switching from elbow flexoion to extension will not be an issue.

Maximal applied force and progression moment are generated in terminal propulsion which is incontrast to the dynamic situation which is characterized by decreasing force in terminal propulsion. However, this can be explained by the different mechanical requirements of the two movement conditions. In the dynamic condition, at initial handrim contact, the upper extremity is just making contact with the handrim, and the applied force is starting from zero. Following hand contactfor the wheel must be accelerated to reach a maximum handrim force in mid-propulsion. Finally, the upper extremity segments must be decelerated by muscle eccentric contraction for re-position in the recovery phase. In the static condition, the the movement requirements do not exist. It can be more feasible to determine the potential musculosketetal performance during different hand position as that appeared in dynamic wheelchair propulsion.

EMG studies have been performed to quantifymuscle activation patterns during wheelchair propulsion in the literature[12, 18]. They found the shoulder flexors (anterior deltoid and pectoralis major) are activated during the most of the propulsion phase. The elbow flexors (long head of biceps brachii) and elbow extensors (triceps brachii) showed a bimodal pattern, the elbow flexor activated in early propulsion and

elbow extensor activated in middle and terminal propulsion phase. They concluded that the shoulder flexors are the primary movers and the elbow flexors and extensors are necessary for an effective force direction [12]. Some investigators analyzed the torque and power output curve during wheelchair propulsion and found a slope change or even a negative declination in the torque curve, during about half of the propulsion phase[12, 16]. This phenomenon could have coincided with the switch in muscular activity from elbow flexor to elbow extensor[12]. Also, this slope declination in middle propulsion may also relate to the findings of this study. The progression moment is smaller in the middle propulsion than that in the initial propulsion. This slope declination pattern could be manifested for increasing the propulsion loading, ex, proposing in the ramp.

A simple 2-D model has already been created. This model will be developed in steps, each with progressively increasing sophistication. The assumptions applied in the initial development of the model will be step-wise relaxed or modified to improve the comparison of the analytic results with the experimental measurements. Wheelchair propulsion involves a fully three-dimensional motion of the upper-extremity and trunk. However, in the initial model development, we feel it is justified to concentrate on the plane of the dominant movement, namely, the sagittal plane. The initial model will be formulated by considering the motions of shoulder flexion

and extension and elbow flexion and extension. Further simulation of wheelchair dynamic propulsion seems have to consider to be based on the minimization of energy losses criterion.

REFERENCE

[1] van der Woude LH, Veeger DJ, Rozendal RH, Sargeant TJ. Seat height in handrim wheelchair propulsion. J Rehabil Res Dev 1989;26:31-50.

[2] Masse LC, Lamontagne M, O'Riain MD. Biomechanical analysis of wheelchair propulsion for various seating positions. J Rehabil Res Dev 1992;29:12-28.

[3] Hughes CJ, Weimar WH, Sheth PN, Brubaker CE. Biomechanics of wheelchair propulsion as a function of seat position and user-to-chair interface. Arch Phys Med Rehabil 1992;73:263-9.

[4] van der Woude LH, Veeger HE, Rozendal RH, van Ingen Schenau GJ, Rooth F, van Nierop P. Wheelchair racing: effects of rim diameter and speed on physiology and technique. Med Sci Sports Exerc 1988;20:492-500.

[5] van der Helm FC, Veeger HE. Quasi-static analysis of muscle forces in the shoulder mechanism during wheelchair propulsion. J Biomech 1996;29:39-52.

[6] Rozendaal LA, Veeger DE. Force direction in manual wheel chair propulsion: balance between effect and cost. Clinical Biomechanics 2000;15:S39-41.

[7] Vanlandewijck Y, Theisen D, Daly D. Wheelchair propulsion biomechanics: implications for wheelchair sports. Sports Med 2001;31:339-67.

[8] Cooper RA. A systems approach to the modeling of racing wheelchair propulsion. J Rehabil Res Dev 1990;27:151-62.

[9] Hofstad M, Patterson PE. Modelling the propulsion characteristics of a standard wheelchair. J Rehabil Res Dev 1994;31:129-37.

[10] Veeger HEJ, Vanderwoude LHV, Rozendal RH. Within-Cycle Characteristics of the Wheelchair Push in Sprinting on a Wheelchair Ergometer. Med Sci Sports Exerc 1991;23:264-71.

[11] Cooper RA, Robertson RN, VanSickle DP, Boninger ML, Shimada SD. Methods for determining three-dimensional wheelchair pushrim forces and moments: a technical note. J Rehabil Res Dev 1997;34:162-70.

[12] Veeger HE, van der Woude LH, Rozendal RH. Within-cycle characteristics of the wheelchair push in sprinting on a wheelchair ergometer. Med Sci Sports Exerc 1991;23:264-71.

[13] Robertson RN, Boninger ML, Cooper RA, Shimada SD. Pushrim forces and joint kinetics during wheelchair propulsion. Arch Phys Med Rehabil 1996;77:856-64.

[14] Boninger ML, Cooper RA, Robertson RN, Shimada SD. Three-dimensional pushrim forces during two speeds of wheelchair propulsion. Am J Phys Med Rehabil 1997;76:420-6.

[15] van der Woude LH, Bakker WH, Elkhuizen JW, Veeger HE, Gwinn T. Propulsion technique and anaerobic work capacity in elite wheelchair athletes: cross-sectional analysis. Am J Phys Med Rehabil 1998;77:222-34.

[16] Veeger HE, van der Woude LH, Rozendal RH. Effect of handrim velocity on mechanical efficiency in wheelchair propulsion. Med Sci Sports Exerc 1992;24:100-7.

[17] van der Woude LH, Veeger HE, Rozendal RH. Propulsion technique in hand rim wheelchair ambulation. Journal of Medical Engineering & Technology 1989;13:136-

41.

[18] Mulroy SJ, Gronley JK, Newsam CJ, Perry J. Electromyographic activity of shoulder muscles during wheelchair propulsion by paraplegic persons. Arch Phys Med Rehabil 1996;77:187-93.

Table 1. Characteristics of subjects participating in the experiment and for the model parameters

Subject	Gender	Age	Height (cm)	Weight (Kg)	Upper arm length (cm)	Forearm length(cm)	Shoulder heigth (cm)
RV	Male	30	183.0	79.7	33.0	34.5	71.0
LG	Male	31	171.0	73.6	33.0	33.0	71.0
MO	Male	40	172.0	87.0	30.0	36.0	68.0
YL	Male	37	170.0	65.1	28.0	34.5	71.0
TT	Male	38	170.0	66.7	27.0	33.0	71.0
Mean	Male	35.2	173.2	74.42	30.2	34.2	70.4

Table 2. Comparisons of the progression moment, force direction and force magnitude between model output and experiment data

Wheel Angle	Progression Moment (N-m)			Force direction (°)			Force Magnitude (N)		
	Model	Experiment	Difference	Model	Experiment	Difference	Model	Experiment	Difference
60°	91.3 (26.3)	44.5 (4.3)	46.8	-60.0 (3.8)	-52.2 (14.1)	-7.8	417.0 (123.7)	139.6 (14.1)	277.4
75°	63.8 (18.0)	42.2 (4.3)	21.6	-63.6 (4.2)	-35.4 (15.7)	-28.2	382.5 (106.7)	184.1 (39.4)	198.4
90°	31.2 (10.7)	38.6 (3.8)	-7.4	0.5 (0.13)	-2.1 (24.5)	2.6	123.0 (42.3)	177.4 (41.1)	-54.4
105°	33.9 (10.0)	42.8 (7.9)	-8.9	18.9 (10.7)	35.6 (20.5)	-16.7	135.3 (38.2)	182.2 (21.8)	-46.9
120°	45.4 (8.9)	52.7 (9.8)	-7.3	84.1 (3.4)	58.3 (16.2)	25.8	308.0 (75.8)	219.7 (69.2)	88.3

Figures Legend

Figure1: Four segment model used for static optimization of wheelchair propulsion. The shoulder (S), elbow (E), and Hand (H) positions are indicated. Vector displacements from the shoulder, elbow, and wheel axle to the hand position are P_S, P_E, and P_r respectively. θ_S, θ_E, and θ_W are the shoulder joint, elbow joint, and wheel angles respectively. Finally, the resultant hand force on the handrim (F_h) as well as its cartesian (F_X, F_Y) and polar coordinates (F_r, F_t) are indicated.

Figure 2a: the isometric shoulder muscle strength and the second order polynominal regression model of flexors (A) and extensors (B) at hyperextension 40 and 20 degrees and shoulder flexion 0, 20, 40, 60 80 degrees with elbow at 90 degree and forearm in neutral position.

Figure 2b: the isometric elbow muscle strength and the second order polynominal regression model of flexors (A) and extensors (B) at elbow flexion 0, 20, 40, 60, 80, 100.and 120 degrees with forearm in neutral position.Figure 3. Mean and standard deviation of handrim force in horizontal (A) and in vertical direction (B) and progression moment (C) during different hand positions

Figure 3. Mean and standard deviation of handrim force in horizontal (A) and in vertical direction (B) and progression moment (C) during different hand positions.

Figure 4a. Stick diagrams of upper extremity and handrim during different hand positions: 120° (A), 105° (B) and 90° (C)

Figure 4b. Stick diagrams of upper extremity and handrim during different hand positions: 75° (A) and 60°

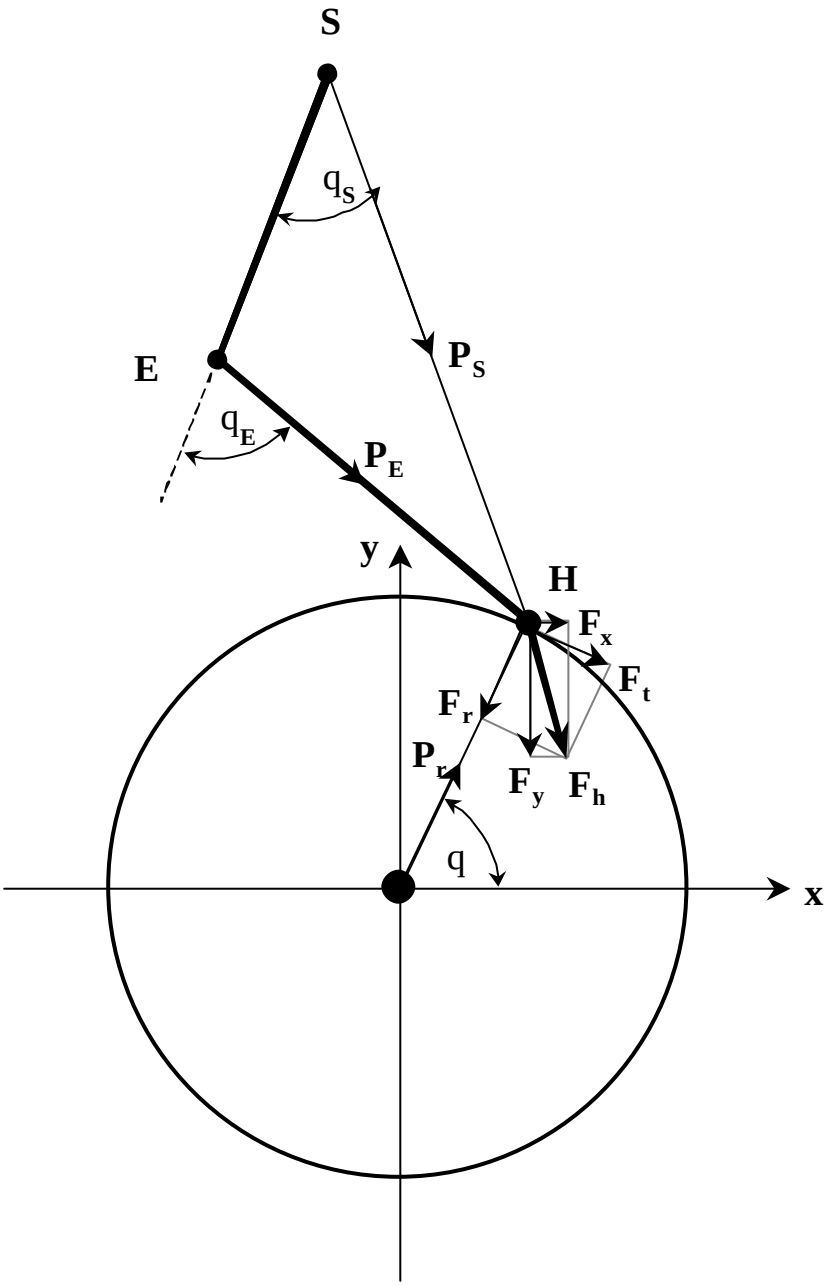

Figure1: Optimization analytic model of wheelchair propulsion mechanics

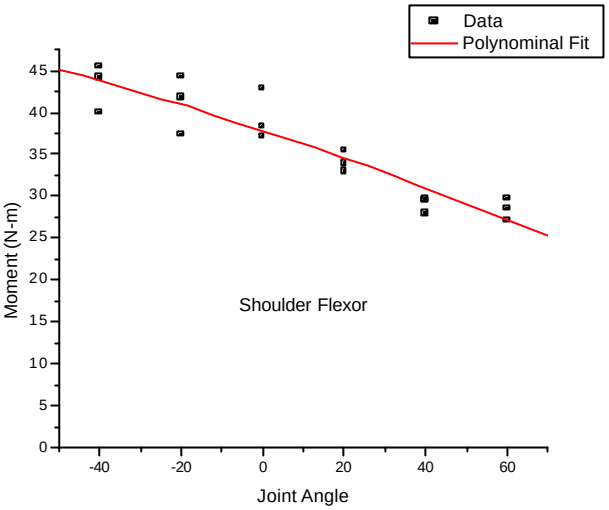

Y = 37.8581 -0.15965 *X -0.000272*X^2

R-Square=0.8605

P<0.0001

(A)

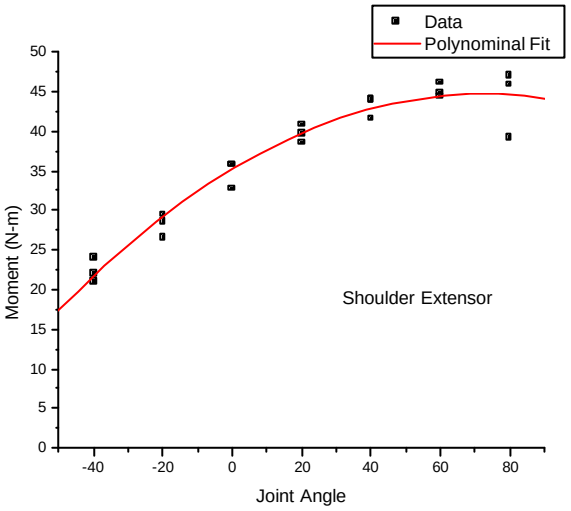

Y = 35.07381 +0.26373*X -0.00181*X^2

R-Square=0.95288

P<0.0001

(B)

Figure 2a: the isometric shoulder muscle strength and the second order polyno minal regression model of flexors (A) and extensors (B) for subject TG at hyp erextension 40 and 20 degrees and shoulder flexion 0, 20, 40, 60 80 degrees with elbow at 90 degree and forearm in neutral position.

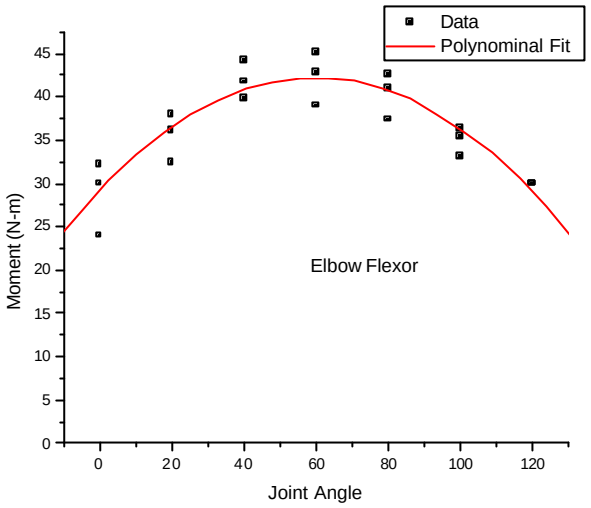

Y = 28.85556 +0.43940*X-0.00364 *X^2

R-Square=0.82172

P<0.0001

(A)

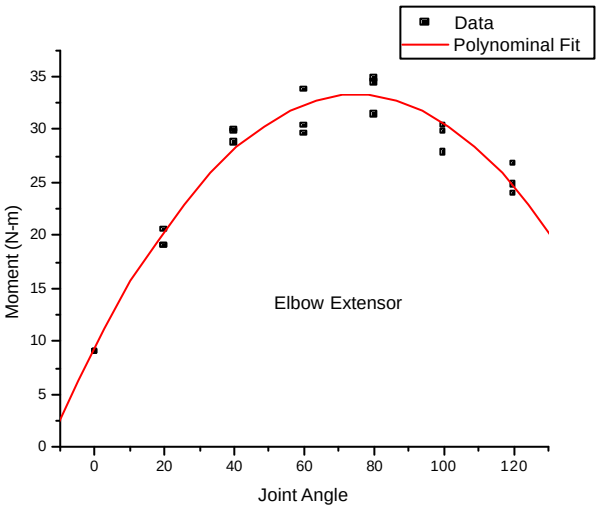

Y = 9.07937 +0.6406*X-0.00426 *X^2

R-Square=0.96615

P<0.0001

(B)

Figure 2b: the isometric elbow muscle strength and the second order polynominal regression model of flexors (A) and extensors (B) for subject TG at elbow flexion 0, 20, 40, 60, 80, 100.and 120 degrees with forearm in neutral position.

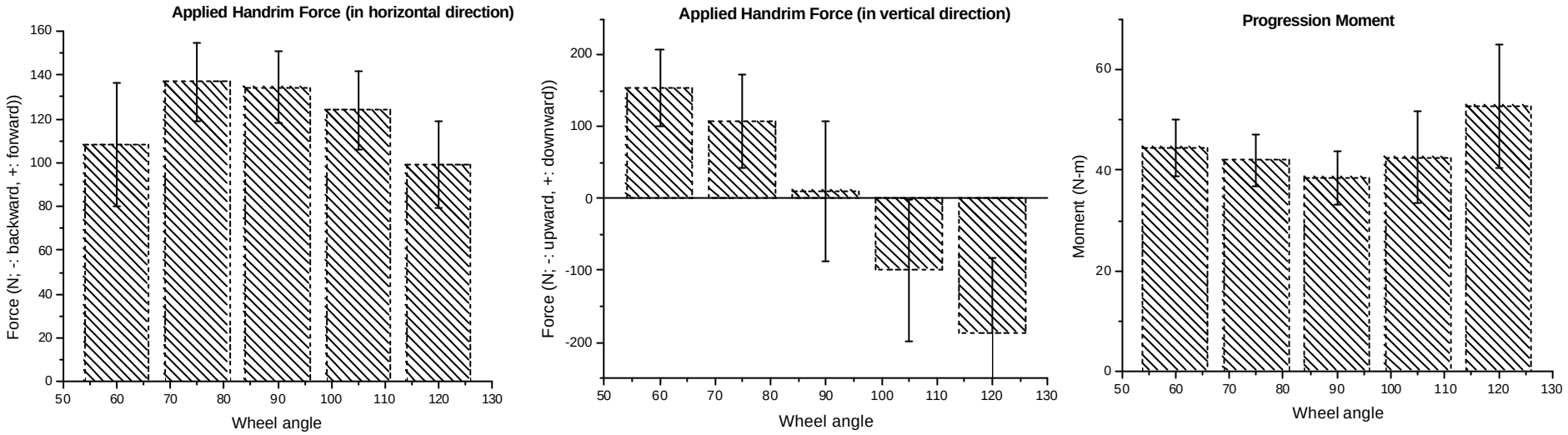

(A) (B) (C)

Figure 3. Mean and standard deviation of handrim force in horizontal (A) and in vertical direction (B) and progression moment (C) during different hand positions.

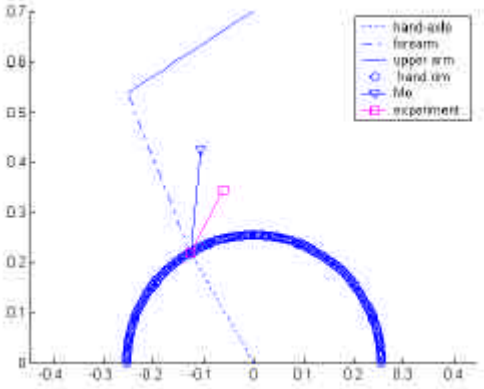

(A)

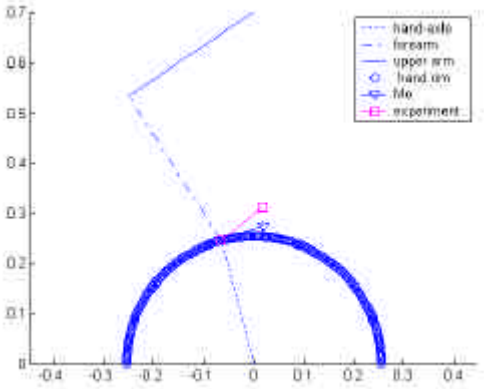

(B)

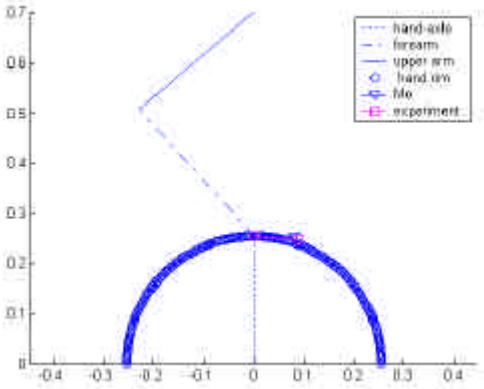

(C)

Figure 4a. Stick diagrams of upper extremity and handrim during different hand positions: 120° (A), 105° (B) and 90° (C)

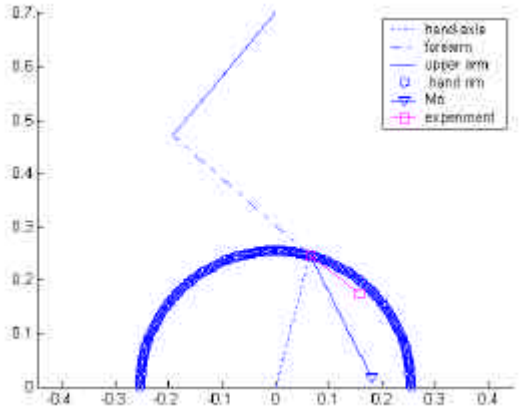

(A)

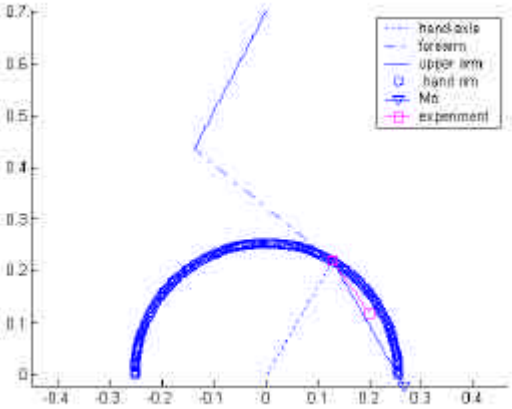

(B)

Figure 4b. Stick diagrams of upper extremity and handrim during different hand positions: 75° (A) and 60°